

# Accelerating Diffusion Transformers with Dual Feature Caching

Chang Zou<sup>1,2</sup>, Evelyn Zhang<sup>1</sup>, Runlin Guo<sup>3</sup>, Haohang Xu<sup>4</sup>,  
 Conghui He<sup>5</sup>, Xuming Hu<sup>6</sup>, Linfeng Zhang<sup>1\*</sup>

<sup>1</sup>Shanghai Jiao Tong University <sup>2</sup>University of Electronic Science and Technology of China

<sup>3</sup>Beijing University of Aeronautics and Astronautics <sup>4</sup>Huawei Technologies Ltd.

<sup>5</sup>Shanghai AI Lab <sup>6</sup>The Hong Kong University of Science and Technology (Guangzhou)

## Abstract

Diffusion Transformers (DiT) have become the dominant methods in image and video generation yet still suffer substantial computational costs. As an effective approach for DiT acceleration, feature caching methods are designed to cache the features of DiT in previous timesteps and reuse them in the next timesteps, allowing us to skip the computation in the next timesteps. However, on the one hand, aggressively reusing all the features cached in previous timesteps leads to a severe drop in generation quality. On the other hand, conservatively caching only the features in the redundant layers or tokens but still computing the important ones successfully preserves the generation quality but results in reductions in acceleration ratios. Observing such a tradeoff between generation quality and acceleration performance, this paper begins by quantitatively studying the accumulated error from cached features. Surprisingly, we find that aggressive caching does not introduce significantly more caching errors in the caching step, and the conservative feature caching can fix the error introduced by aggressive caching. Thereby, we propose a dual caching strategy that adopts aggressive and conservative caching iteratively, leading to significant acceleration and high generation quality at the same time. Besides, we further introduce a V-caching strategy for token-wise conservative caching, which is compatible with flash attention and requires no training and calibration data.

Our codes have been released in Github:

Code: <https://github.com/Shenyi-Z/DuCa>

## 1. Introduction

Diffusion Models (DMs)[16] have shown remarkable success in both image [27] and video generation [2]. Traditional DMs often use U-Net denoising structures, such as Stable Diffusion (SD)[27] and Stable Video Diffusion

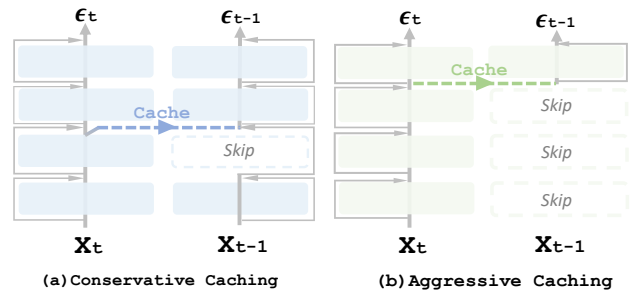


Figure 1. Comparison between conservative caching (a) and aggressive caching (b): Conservative caching skips fewer layers than aggressive caching to maintain the generation quality, but also leads to lower acceleration ratios.  $t$  and  $t-1$  denote the refreshing and caching timesteps, respectively.

(SVD)[2], which have already demonstrated impressive results. Most recently, with the introduction of Diffusion Transformers (DiT)[26], the quality of visual generation has further significantly improved, propelling the development of numerous downstream applications [12]. However, the quality improvement is also accompanied by a significant increase in computational demands, reducing the inference efficiency of transformers and making their deployment in practical scenarios a pressing challenge.

Recently, feature caching has become one of the most popular techniques for diffusion acceleration. Motivated by the high similarity between features in the adjacent timesteps, *aggressive* feature caching caches the features computed in a *freshing timestep*, and then reuses them in the following several *caching steps*, as shown in Figure 1(b). Such a fresh-then-cache strategy enables the diffusion model to save computational costs in the caching step and thus leads to significant acceleration. However, since the similarity of features in non-adjacent timesteps decreases quickly, the error introduced by aggressive feature caching can be accumulated at an exponential speed, leading to a significant drop in generation quality, and making aggressive feature caching impractical.

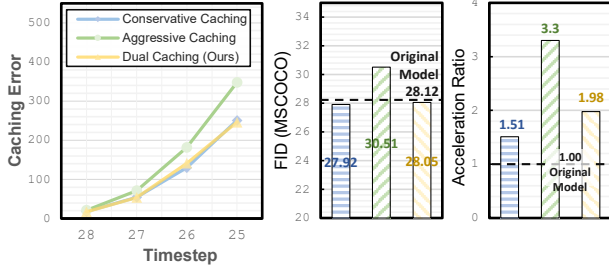


Figure 2. The caching error and acceleration ratio of three feature caching strategies. The caching error is defined as the  $L_2$ -norm distance between  $x_t$  computed with and without feature caching.

To solve this problem, recent works [8, 24, 28, 35] introduce a few computations during the caching steps in certain layers and tokens, which make the cached features in previous steps be corrected for the current caching step. These conservative feature caching methods reduce the accumulated error from feature caching but also make it difficult to achieve a higher acceleration ratio. Such a tradeoff between acceleration ratio and generation quality becomes the most essential problem for feature caching methods.

To investigate this issue, we first examine the performance of conservative caching methods and the aggressive caching method quantitatively. As shown in Figure 2, we observe that the caching error from conservative caching methods increases at a relatively slower rate as the caching step grows, while the error in the aggressive caching method accumulates rapidly with each additional caching step, which explains the aforementioned tradeoff. Notably, we find that the caching error of the aggressive and conservative caching exhibit a close value at the first caching step (*i.e.*, timestep 27 in Figure 2) but a significantly larger value in the following caching steps, suggesting that it is possible to have high acceleration ratios and generation quality by leveraging both cache schemes at appropriate caching steps.

Based on this observation, we propose **DUAL CACHING**, which leverages the advantages of aggressive and conservative caching methods. In each caching cycle, **DuCa** first initializes the cache by performing the full computation in the *fresh* timestep. Then, it performs the one-step aggressive caching for high-ratio acceleration, followed by one-step conservative caching to fix the cache error. Such an alternative caching strategy can be repeated multiple times.

In addition, we further introduce a token-wise caching method as our conservative caching strategy. Token-wise feature caching has been recently proposed to perform computation for only the important tokens in the caching steps. However, the definition of important tokens in the previous work [35] relies on the attention weights in self-attention, making it not compatible with FlashAttention[9] and memory-efficient attention. This problem further improves the memory costs of attention from  $O(N)$  to  $O(N^2)$ ,

also resulting in additional latency, making it not applicable. To address this issue, we introduce **V-Caching**, which approximates the attention weight-based importance score by the norm of the value matrix, providing good compatibility with FlashAttention and memory-efficient Attention while maintaining good generation quality.

Extensive experiments have demonstrated the performance of our method in abundant benchmarks, including text-to-image generation with PixArt- $\alpha$ , text-to-video generation with OpenSora, and class-conditioned image generation with DiT. For instance,  $1.98\times$  acceleration on PixArt- $\alpha$  and  $2.50\times$  acceleration on OpenSora with almost no loss on generation quality.

In summary, our main contributions are as follows:

1. We study the caching error for aggressive feature caching and conservative feature caching, and introduce **DuCa**, a dual feature caching strategy to perform the two caching methods alternatively, maintaining the generation quality while achieving a higher acceleration ratio.
2. We introduce **V-caching** as the conservative caching strategy in **DuCa**, a token-wise feature caching strategy that selects the important tokens via the norm of their value matrix, making it compatible with FlashAttention[9].
3. Extensive experiments have demonstrated **DuCa** in conditional image generation, text-to-image generation, and text-to-video generation, outperforming previous methods by a large margin. Our codes have been released.

## 2. Related Works

**Transformers in Diffusion Models** Diffusion Models (DMs)[16, 30] generate images by gradually adding noise to the image during training and iteratively applying a denoising model to a randomly initialized noise during inference. DMs have recently gained extensive application across various tasks in image generation due to their outstanding performance [1, 27]. Earlier DMs with U-Net-based architectures [16, 27], which also include some Transformer layers, have achieved impressive results. Recently, Diffusion Transformer (DiT) [26] has been constructed by directly stacking multiple DiT Blocks in a cascade, achieving performance in class-conditional image generation that surpasses U-Net-based DMs. Consequently, the DiT architecture has been further extended to several generative fields, yielding exceptional outcomes. For example, the PixArt series [5–7] and similar text-to-image models incorporate Cross-Attention into the DiT Block to add text conditional information into generation procedure, while the Sora series [4, 18] enhances the DiT Block’s Attention structure to Spatial-Temporal attention, enabling high-quality video generation. However, though success, these DiT-based DMs also entail significantly higher computational costs and time consumption, making deploying such

generative models in real-world applications challenging.

**Acceleration of Diffusion Models** To address the high computational costs commonly associated with DMs including DiT, various acceleration methods have been proposed. Existing acceleration methods can generally be divided into two categories: Designing sampling methods to reduce the number of steps needed to transition from noise to high-quality images, and directly accelerating the denoising model. Sampling-based acceleration methods enhance the efficiency of DMs by simply reducing the sampling steps. DDIM [31] leverages a deterministic, non-Markovian reverse process to significantly reduce generation steps while maintaining high-quality outputs. DPM Solver [22], through analytic derivation, optimizes the reverse process, enabling efficient sampling with fewer steps, while DPM Solver++ [23] further refines this approach by incorporating noise control and diverse sampling techniques to improve quality and adaptability. Rectified Flow [21] employs a recurrent flow framework, utilizing specially designed flow fields to accelerate the diffusion process.

**Feature Caching** Methods that improve generation efficiency by accelerating the denoising model largely vary depending on the model structure. Acceleration methods for denoising models in different aspects have been proposed and work well, including weight quantization [29], structural pruning [11], knowledge distillation [19] and token merge [3]. Due to the high computational cost of retraining the diffusion models, or even small learnable modules introduce significant costs, limiting model reusability across different scales, resolutions, and tasks, driving interest in training-free acceleration methods. Faster Diffusion [27] improves computational efficiency by caching the output of the encoder module on certain steps, while DeepCache [25] reduces redundant computations by reusing low-resolution feature information in the skip connections of the U-Net structure. Unfortunately, although both are training-free methods, they are specialized feature caching techniques designed specifically for U-Net-based models like Stable Diffusion [27], making them difficult to directly adapt to transformer-based models like DiT [8]. Recently, to address the lack of feature reuse solutions for DiT,  $\Delta$ -DiT [8] and Pyramid Attention Broadcast (PAB) [33] have been introduced. The former focuses on constructing residuals of DiT outputs across different layers, while the latter emphasizes the importance of various types of attention within DiT Blocks containing multiple attention heads. Learning-to-Cache [24] achieves higher acceleration ratios by employing a learnable router to determine whether computations are needed at each layer, but it incurs prohibitive computational costs. These feature caching methods generally lack attention to finer-grained features. ToCa [35] proposes a method that selects important tokens at both layer and token granularity, allocating more computation to these to-

kens while caching less important ones, advancing temporal redundancy management to the token level.

*The errors introduced by feature caching are primarily attributed to discrepancies in timestep-sensitive information.* Comparing the feature caching methods for DiT discussed above, we find that these feature caching approaches for DiT employ different types of feature cache-reuse structures, resulting in significant variations in acceleration ratios while maintaining generation quality. Additionally, they commonly introduce additional computations to mitigate and correct the discrepancies between cached features and the requirements of the current time step. Our proposed method DuCa demonstrates that *conservative* architectures like ToCa, with their long-range feature reuse capability, can correct timestep information for *aggressive* methods that struggle with larger timestep intervals. By leveraging the high caching ratios of *aggressive* methods, DuCa further enhances acceleration efficiency.

### 3. Method

#### 3.1. Preliminary

**Diffusion Models** Diffusion models [16] are designed with two main processes: a forward process, where Gaussian noise is incrementally added to a clean image, and a reverse process, where a standard Gaussian noise is gradually denoised to reconstruct the original image. Letting  $t$  represent the timestep and  $\beta_t$  the noise variance schedule, the conditional probability in the reverse (denoising) process,  $p_\theta(x_{t-1} | x_t)$ , can be modeled as:

$$\mathcal{N}\left(x_{t-1}; \frac{1}{\sqrt{\alpha_t}}\left(x_t - \frac{1 - \alpha_t}{\sqrt{1 - \bar{\alpha}_t}}\epsilon_\theta(x_t, t)\right), \beta_t \mathbf{I}\right), \quad (1)$$

where  $\alpha_t = 1 - \beta_t$ ,  $\bar{\alpha}_t = \prod_{i=1}^T \alpha_i$ , and  $T$  represents the total number of timesteps. Notably,  $\epsilon_\theta$  is a denoising network parameterized by  $\theta$ , which takes  $x_t$  and  $t$  as the inputs to predict the noise needed for denoising. In an image generation procedure using  $\mathcal{T}$  timesteps,  $\epsilon_\theta$  must perform inference  $\mathcal{T}$  times, which constitutes the majority of computational costs in diffusion models. Recently, numerous studies have shown that implementing  $\epsilon_\theta$  as a transformer often enhances generation quality.

**Diffusion Transformers** Diffusion transformers (DiT) are usually composed of stacking groups of self-attention layers  $\mathcal{F}_{SA}$ , multilayer perceptron  $\mathcal{F}_{MLP}$ , and cross-attention layers  $\mathcal{F}_{CA}$  (for conditional generation). It can be roughly formulated as:

$$\mathcal{G} = g_1 \circ g_2 \circ \dots \circ g_L, \quad \text{where} \quad (2)$$

$$g_l = \mathcal{F}_{SA}^l \circ \mathcal{F}_{CA}^l \circ \mathcal{F}_{MLP}^l,$$

$\mathcal{G}$ ,  $g_l$ , and  $\mathcal{F}^l$  represent the DiT model, the blocks in DiT, and different layers in a DiT block, respectively.  $l$  denotes

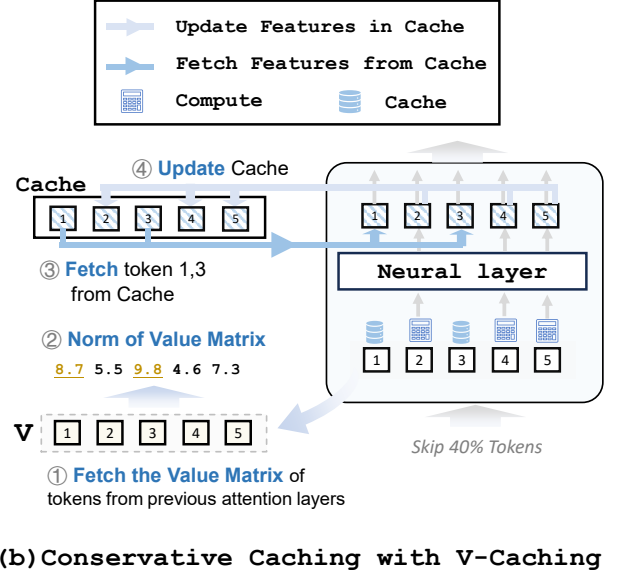
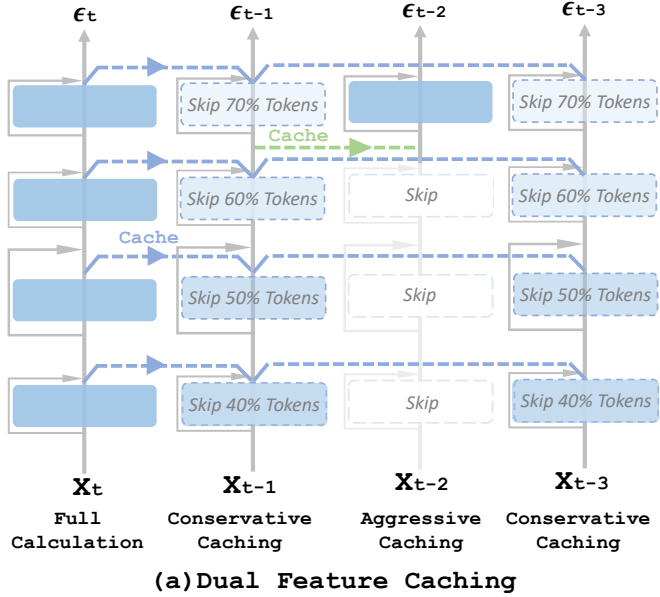


Figure 3. The overview of DuCa. (a) In the first timestep of a cache cycle, DuCa computes all tokens and stores them in the cache as initialization. Then, DuCa performs a conservative caching step followed by an aggressive caching step, and then another conservative caching step, alternating in this manner to form a complete cache cycle. (b) The proposed V-Caching method selects important tokens for DuCa by first fetching the value matrix for all input tokens that have been previously computed in the attention layers and then computing the norm of the value matrix for each token. The tokens with the largest V-norm values are selected as cached tokens. The computation results for these tokens are directly retrieved from the cache, while the remaining tokens are computed through the neural layer, with their updated results stored back into the cache.

the index of DiT blocks and  $L$  denotes the depth of DiT. In diffusion transformers, the input data  $\mathbf{x}_t$  consists of a sequence of tokens representing different patches in the generated images, expressed as  $\mathbf{x}_t = \{x_i\}_{i=1}^{H \times W}$ , where  $H$  and  $W$  indicate the height and width of the images or their latent code, respectively. Then, the computation between  $\mathcal{F}$  and  $\mathbf{x}$  can be generally written as  $\mathcal{F}(\mathbf{x}) = \mathbf{x} + \text{AdaLN} \circ f(\mathbf{x})$ , where the first item  $\mathbf{x}$  indicates the residual connection and  $f$  denotes the MLP or attention layers. AdaLN indicates the adaptive layer normalization [13].

**Feature Caching:** Feature caching aims to reuse the features that are computed and cached in the past timesteps to skip the computation in future timesteps. It is usually performed in multiple repeated caching cycles. Assuming a caching cycle with  $N$  timesteps from the timestep  $t$  to  $t + N - 1$ , then feature caching performs the full computation in the timestep  $t$  and stores the obtained features in a cache. This progress can be denoted as  $\mathcal{C}[l] := g_l(x_t)$ , where  $\mathcal{C}$  denotes the cache and “:=” denotes assigning value operation. Then, in timesteps from  $t + 1$  to  $t + N - 1$ , the computation in these steps is skipped by reusing the cached features, which can be formulated as  $g_l(x_{t+i}) := \mathcal{C}[l], i \leq N - 1$ . For simplicity, in this paper, the timestep  $t$  and the timesteps in  $[t + 1, t + N - 1]$  are named the *freshing step* and the *caching steps*, respectively.

### 3.2. Dual Feature Caching

The proposed dual feature caching aims to perform aggressive caching and conservative caching alternatively in the caching steps. Hence, in this section, we first introduce the details of the two caching strategies.

**Aggressive Caching in DuCa** As introduced in Figure 1(b), aggressive caching directly replaces the output of the DiT block with the cached feature which is computed in previous layers, which means that all computations of the first  $l$  layers can be skipped. This can be expressed as  $g_l := \mathcal{C}[l]$ , where  $\mathcal{C}[l]$  denotes the cached feature at the  $l$ th layer. Then, the computation with aggressive caching can be written as:

$$\mathcal{G}(x)_t := g_{l+1} \circ \dots \circ g_L^t(\mathcal{C}[l]). \quad (3)$$

To achieve the maximal acceleration with aggressive caching, we set  $l = L - 1$  in most of our experiments, which indicates almost skipping all the layers in the caching step.

**Conservative Caching in DuCa** As shown in Figure 1(a), conservative caching does not cache and reuse all the features. Instead, it caches and reuses only the features without the residual connection, which allows it to allocate the computation to some layers in the caching steps to correct the cached features. Recently, ToCa [35] introduced a token-wise approach that selectively reuses features based on the

importance of each token and its sensitivity to caching, which enables us to perform computation only in the important tokens. Following ToCa, we first calculate an importance score  $\mathcal{S}$  for each token  $x_i$  and then use this score to divide the index set of tokens  $\mathcal{I}$  into two *complementary* sets:  $\mathcal{I}_{\text{Cache}}$ , for tokens to be cached, and  $\mathcal{I}_{\text{Compute}}$ , for tokens to be computed. Subsequently, the computation for the  $i_{th}$  token  $x_i$  on the  $l_{th}$  layer can be expressed as:

$$\gamma_i f^l(x_i) + (1 - \gamma_i) \mathcal{C}[l](x_i), \quad (4)$$

where  $\gamma_i = 0$  for  $i \in \mathcal{I}_{\text{Cache}}$  and  $\gamma_i = 1$  for  $i \in \mathcal{I}_{\text{Compute}}$ . Here,  $\mathcal{C}[l](x_i)$  denotes retrieving the cached value of  $x_i$  from the conservative cache  $\mathcal{C}$  at layer  $l$ , which incurs no computation cost, enabling partial omission of calculations. After this selective computation in the token dimension, the computed features are updated to  $\mathcal{C}[l]$  for future reusing.

**Value-based Token-wise Feature Caching:** As the previous token-wise conservative caching method, ToCa offers two attention map-based selection strategies that have shown good effectiveness. However, the attention map-based selection strategy is incompatible with another commonly used attention-optimization method FlashAttention[9] and memory-efficient attention, which can not provide the attention scores but are capable of reducing the memory costs of attention from  $O(N^2)$  to  $O(N)$  and significant accelerating the attention layers. This conflict between attention scores-based token selection with this optimized attention computation makes ToCa less practical in application and raises the requirements for attention score-free token selection methods.

Figure 4 shows the relation between the norm of the value matrix and the attention scores of each token, which demonstrates that tokens with high attention scores in the self-attention map tend to have relatively smaller norms in their value matrix. This suggests that we can directly select tokens with smaller norms in their value matrix as substitutes for those with high attention map scores. Concretely, the value matrix of each token is produced by a linear layer in attention layers as follows:  $v_i = \text{MLP}_v(x_i)$ , where  $v_i$  is value vector for the  $i^{th}$  token. Therefore, V-Caching gives the selection rule for  $\mathcal{I}_{\text{Cache}}$  as follows:

$$\mathcal{I}_{\text{Cache}} = \arg \max_{\{i_1, i_2, \dots, i_n\} \subseteq \{1, 2, \dots, N\}} \{\|v_{i_1}\|_2, \|v_{i_2}\|_2, \dots, \|v_{i_n}\|_2\}, \quad (5)$$

where the  $n$  is the total number of selected tokens, defined by  $n = \lfloor R\% \times N \rfloor$ .

### 3.3. Overall Framework

Built on the deeper understanding of aggressive and conservative caching, DuCa introduces a caching scheme that alternates conservative and aggressive caching in different

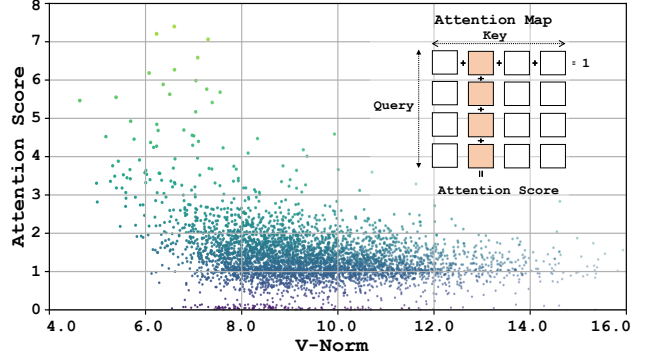


Figure 4. The relation between the self-attention score and the norm of the value matrix for each token. Tokens with the largest attention score tend to have a lower norm in the value matrix.

steps. V-Caching serves as the conservative caching strategy, as shown in Figure 3. This design leverages the realignment capability of token-wise conservative caching to correct the misaligned timestep information occurring in aggressive caching steps. Therefore, it enables the high local compression rate of aggressive caching to be applied to more steps while further reducing redundant computations in conservative caching steps. In practice, we arrange token-wise conservative caching steps on odd-numbered steps following a fresh step, and aggressive caching steps on even-numbered steps.

## 4. Experiments

### 4.1. Experiment Settings

#### 4.1.1. Model Configurations

Experiments are conducted on three widely known DiT-based models on the three generation tasks with the correlating default samplers, including PixArt- $\alpha$  [7] with 20 DPM Solver++ [23] steps for text-to-image generation, OpenSora [34] with 30 reflected flow steps [21] for text-to-video generation, and DiT-XL/2 [26] with 50 DDIM [31] steps for class-conditional image generation. All the experiments are conducted with NVIDIA H800 80GB GPUs. See More details in our appendix.

#### 4.1.2. Evaluation and Metrics

**Text-to-image generation** We randomly select 30,000 captions from COCO-2017 datasets [20] to generate the 30,000  $256 \times 256$  images. **FID-30k** is computed using the 30k generated images and the real images from COCO-2017 to evaluate the quality of text-to-image generation. Besides, the **CLIP** score [14] is computed between the 30k prompt-image pairs to evaluate the text-image alignment. All the CLIP scores are tested using the Vit-large-14 model.

**Text-to-video generation VBench** [17] evaluation framework is applied to evaluate the performance of the text-to-video model. With 5 videos per prompt and 950 prompts

Table 1. **Quantitative comparison of text-to-image generation** on MS-COCO2017 with PixArt- $\alpha$  and 20 DPM++ sampling steps.

Method	Latency(s)↓	FLOPs(T)↓	Speed↑	MS-COCO2017 FID-30k↓	CLIP↑
PixArt- $\alpha$ [7]	0.242	11.88	1.00×	28.12	16.29
50% steps	0.121	5.94	2.00×	37.57	15.83
FORA [28]	0.178	5.66	1.98×	29.67	16.40
ToCa[35]	0.167	6.05	1.96×	28.38	16.43
DuCa(C-A score)	0.157	5.99	1.98×	<b>27.98</b>	<b>16.44</b>
DuCa(V-Caching)	<b>0.088</b>	5.99	1.98×	28.05	16.42

Table 2. **Quantitative comparison in text-to-video generation** on VBench. \*Results are from PAB [33]. PAB<sup>1-3</sup> indicate PAB with different hyper-parameters.

Method	Latency(s)↓	FLOPs(T)↓	Speed↑	VBench(%)↑
OpenSora [34]	54.83	3283.20	1.00×	79.41
$\Delta$ -DiT* [8]	53.45	3166.47	1.04×	78.21
T-GATE* [32]	45.91	2818.40	1.16×	77.61
PAB <sup>1*</sup> [33]	41.05	2657.70	1.24×	78.51
PAB <sup>2*</sup> [33]	39.96	2615.15	1.26×	77.64
PAB <sup>3*</sup> [33]	38.26	2558.25	1.28×	76.95
50% steps	28.85	1641.60	2.00×	76.78
FORA [28]	33.19	1751.32	1.87×	76.91
ToCa[35]	29.03	1394.03	2.36×	78.59
DuCa(C-A score)	26.77	1315.62	<b>2.50×</b>	<b>78.63</b>
DuCa(V-Caching)	19.16	1315.62	2.50×	78.54

from the framework, 4,750 videos are generated to evaluate the 16 aspects proposed by VBench. The generated videos are 480p, 9:16, and 2s videos.

**Class-conditional image generation** 50,000  $256 \times 256$  images uniformly sampled from the 1,000 classes in ImageNet[10] are generated to evaluate the FID-50k [15]. Besides, sFID, Precision, and Recall are introduced as supplementary metrics.

## 4.2. Quantitative and Qualitative Results

### 4.2.1. Results on text-to-image generation

As shown in Table 1, we compared the DuCa under two different token selection methods: Cross-Attention score from ToCa and the proposed V-norm score with three training-free acceleration methods: ToCa[35], the 10 DPM++ sampling steps and FORA [28], a layer-wise conservative caching method.

In terms of *generation quality*, the quantitative results demonstrate that under an acceleration ratio close to 2.0, the DuCa methods achieve the lowest FID-30k score on the MS-COCO2017 generation task, with almost no loss in generation quality compared to the original non-accelerated approach. For instance, the DuCa method using the Cross-Attention score reduces the FID-30k by 0.40 compared to the ToCa method with the same acceleration ratio, while the DuCa method using the V-norm score also decreases the FID-30k by 0.33, demonstrating that our alternating ac-

celeration strategy effectively enhances generation quality.

In terms of evaluating the *text-image alignment* metric, the performance of the DuCa method is very close to that of ToCa and generally superior to the approach of directly setting 50% generation steps. For example, the DuCa method with Cross-Attention score and V-norm score achieves CLIP scores on MS-COCO2017 that are 0.61 and 0.59 higher, respectively, compared to the 50% generation steps method with the same acceleration ratio. These scores are even slightly better than those of the original non-accelerated PixArt- $\alpha$  model, with improvements of 0.15 and 0.13, respectively, demonstrating better controllability.

In addition, thanks to the acceleration brought by the compatibility with FlashAttention [9], the latency of the DuCa method with V-norm score is reduced by 0.069 compared to the DuCa method with Attention score, representing an approximate 43.9% reduction, which is a significant improvement in acceleration.

### 4.2.2. Results on text-to-video generation

The generation results of  $\Delta$ -DiT, T-GATE[32], PAB[33], 15 rflow sampling steps, ToCa[35], FORA [28] and proposed DuCa on the text-to-video model OpenSora[34] are shown in Table 2.

As shown in Table 2, DuCa achieves a further acceleration from  $2.36 \times$  (as with ToCa) to  $2.50 \times$  with virtually no loss in generation quality. Additionally, despite having the lowest computational cost among all the compared methods, DuCa still achieves the highest VBench score. This demonstrates that the proposed strategy in DuCa, which alternates between aggressive and conservative caching steps, effectively eliminates the redundant components present in a fully conservative caching approach.

Additionally, comparing the generation results of the Cross-Attention and V-Caching token selection strategies, we only observe a slight decrease of 0.09 in the VBench score with the V-Caching strategy. More significantly, V-Caching reduces generation time by 7.61 seconds, approximately 28.4%. This indicates that DuCa effectively leverages V-Caching to make the acceleration method compatible with FlashAttention[9], achieving substantial reductions in generation time. In practice, using V-Caching will be more advantageous for rapid inference.

In Figure 7, we further present the performance of DuCa and the aforementioned methods across various dimensions of the VBench metric. DuCa shows results consistent with the non-accelerated original OpenSora model across multiple metrics, including but not limited to Overall Consistency, Temporal Style, Scene, and Object Class. Additionally, the Cross-Attention and V-Caching strategies introduce only a slight difference in Spatial Relationship, further underscoring the exceptional performance of DuCa and the proposed V-Caching in practical scenarios.

Table 3. Quantitative comparison on class-to-image generation on ImageNet with DiT-XL/2.

Method	Latency(s) ↓	FLOPs(T) ↓	Speed ↑	sFID ↓	FID ↓	Precision ↑	Recall ↑
DiT-XL/2-G (cfg = 1.50)	2.012	118.68	1.00×	4.98	2.31	0.82	0.58
DDIM-50 steps	0.417	23.74	1.00×	4.40	2.43	0.80	0.59
DDIM-25 steps	0.209	11.87	2.00×	4.74	3.18	0.79	0.58
DDIM-20 steps	0.167	9.49	2.50×	5.15	3.81	0.78	0.58
DDIM-17 steps	0.142	8.07	2.94×	5.76	4.58	0.77	0.56
FORA [28]	0.197	4.29	2.77×	6.43	3.88	0.79	0.54
ToCa(a)	0.195	8.73	2.72×	5.14	3.64	0.79	0.55
ToCa(b)	0.214	10.23	2.32×	4.70	3.05	0.79	0.57
DuCa(a)(S-A score)	0.184	8.76	2.71×	4.66	3.19	0.79	0.57
DuCa(b)(S-A score)	0.200	9.58	2.48×	<b>4.66</b>	<b>3.05</b>	0.80	0.57
DuCa(a)(V-Caching)	<b>0.177</b>	<b>8.76</b>	2.71×	4.68	3.19	0.80	0.57
DuCa(b)(V-Caching)	0.198	9.58	2.48×	4.69	3.06	0.80	0.57

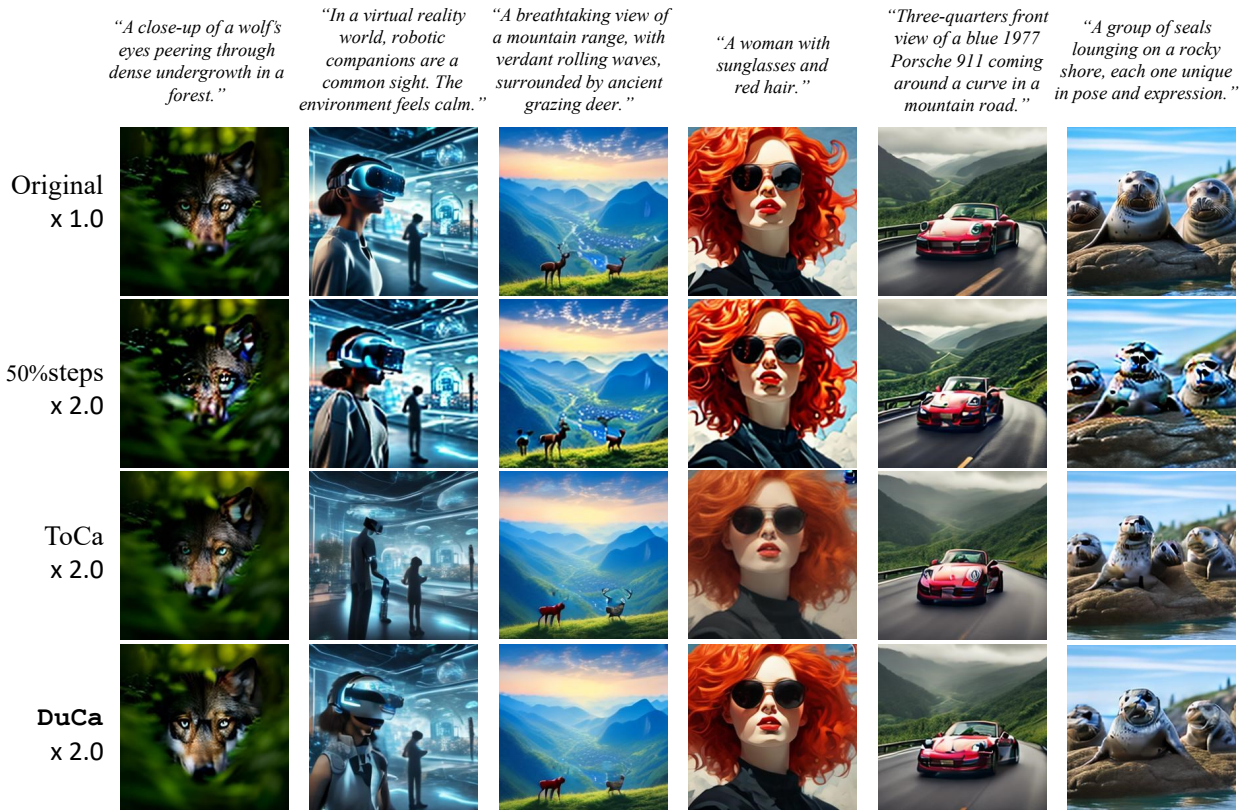


Figure 5. Visualization results for different acceleration methods on PixArt- $\alpha$ .

#### 4.2.3. Results on class-conditional image generation

In Table 3, we compare ToCa[35], FORA [28], the direct reduction of corresponding DDIM steps, and the proposed DuCa under Self-Attention score and V-Caching token selection strategies. The experimental results indicate that with comparable FID scores, representing generation quality, DuCa further enhances acceleration. For instance, DuCa(b) with Self-Attention score achieves a similar FID-50k as ToCa(b), but the acceleration ratio increases from 2.36 to 2.48. Additionally, under a higher acceleration sce-

nario with an acceleration ratio around 2.7, DuCa achieves an FID-50k of 3.19, further reducing the FID-50k by 0.45 compared to ToCa’s 3.64. This demonstrates that DuCa effectively reallocates computation to more critical areas.

#### 4.3. Ablation Studies

As shown in Table 4, we compare Random, Cross-Attention based, and V-Caching token selection methods on PixArt- $\alpha$  in terms of latency, FLOPs, FID-30k, and CLIP score. It can be observed that the cross-Attention-based selection

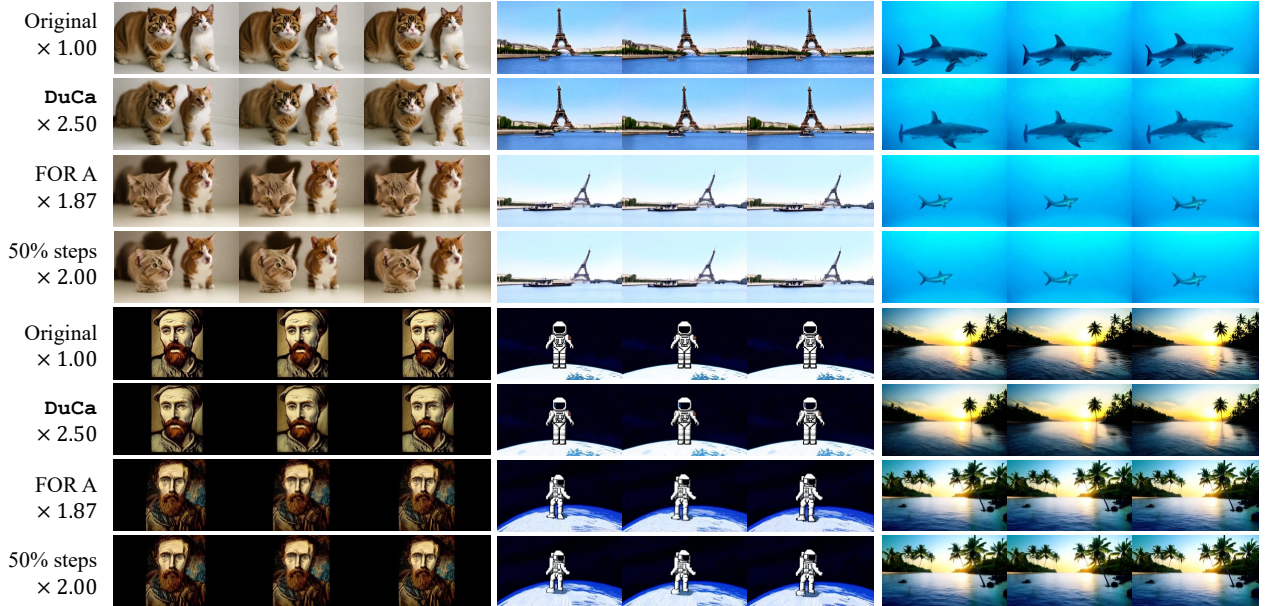


Figure 6. Visualization results for different methods on OpenSora (videos available in the supplementary material).

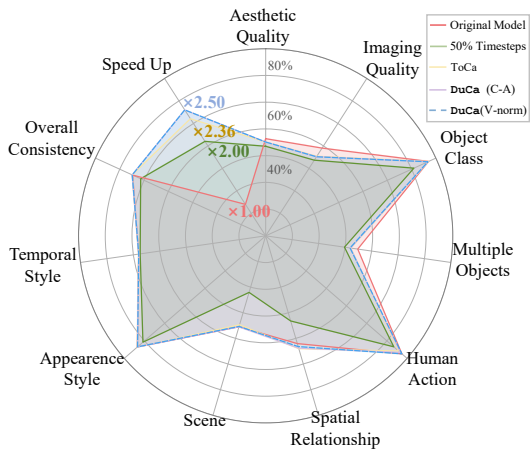


Figure 7. VBench metrics and acceleration ratio of proposed DuCa and other methods

Table 4. Ablation Study for different token selection methods for DuCa on PixArt- $\alpha$ .

Methods	MS-COCO2017		Latency(s) ↓ FLOPs(T) ↓	
	FID-30k ↓	CLIP ↑		
<b>Random</b>	28.34	16.42	0.089	5.99
<b>Cross-Attention</b>	<b>27.98</b>	<b>16.44</b>	0.157	5.99
<b>V-Caching</b>	28.05	16.42	<b>0.088</b>	5.99

Table 5. Comparison on different caching methods on PixArt- $\alpha$ .

Methods	MS-COCO2017		FLOPs(T) ↓
	FID-30k ↓	CLIP ↑	
<b>Conservative-only</b>	<b>27.92</b>	16.39	7.84
<b>Aggressive-only</b>	30.51	16.39	3.59
<b>DuCa</b>	28.05	<b>16.42</b>	5.99

method achieves the best performance in generation quality and text-image alignment, but due to its incompatibility with FlashAttention[9], its latency is as high as 0.157 seconds—nearly twice that of V-Caching and Random selection. In contrast, V-Caching achieves nearly the same, only slightly lower, FID-30k and CLIP scores, along with faster generation speed. Despite the minimal impact of the three token selection methods on computational load, the FlashAttention[9]-compatible V-Caching method shows significantly higher acceleration due to computational optimizations. Thus, V-Caching stands out as a superior generation scheme that effectively balances quality and efficiency.

As shown in Table 5, we compare the Conservative-only, Aggressive-only, and alternating DuCa structures on PixArt- $\alpha$  in terms of FLOPs, FID-30k, and CLIP score. The Conservative-only structure appears to have the best generation quality but incurs an excessively high computational cost. In contrast, Aggressive-only reduces computation to nearly half of Conservative-only but suffers significantly in generation quality. Our proposed DuCa structure achieves a computational load between the two, with only a slight 0.13 increase in FID-30k compared to the high-computation Conservative-only approach, while improving text-image alignment. This indicates that DuCa effectively eliminates most redundant computation present in Conservative-only.

## 5. Conclusion

This paper first gives an in-depth study of the caching error on aggressive and conservative methods, and then introduces dual caching DuCa, which performs aggressive and conservative alternatively to leverage their advantages in different caching steps. Besides, V-Caching is introduced

to perform token-wise conservative caching based on the norm of the value matrix of the tokens, making it compatible with default optimized attention computation such as FlashAttention, allowing feature caching to be practical in real applications. We hope this paper can attract more attention to feature caching for its real benefits, to make it simple but effective, instead of being complex.

## References

- [1] Yogesh Balaji, Seungjun Nah, Xun Huang, Arash Vahdat, Jiaming Song, Qinsheng Zhang, Karsten Kreis, Miika Aittala, Timo Aila, Samuli Laine, et al. ediff-i: Text-to-image diffusion models with an ensemble of expert denoisers. *arXiv preprint arXiv:2211.01324*, 2022. 2
- [2] Andreas Blattmann, Tim Dockhorn, Sumith Kulal, Daniel Mendelevitch, Maciej Kilian, Dominik Lorenz, Yam Levi, Zion English, Vikram Voleti, Adam Letts, et al. Stable video diffusion: Scaling latent video diffusion models to large datasets. *arXiv preprint arXiv:2311.15127*, 2023. 1
- [3] Daniel Bolya and Judy Hoffman. Token merging for fast stable diffusion. In *Proceedings of the IEEE/CVF conference on computer vision and pattern recognition*, pages 4599–4603, 2023. 3
- [4] Tim Brooks, Bill Peebles, Connor Holmes, Will DePue, Yufei Guo, Li Jing, David Schnurr, Joe Taylor, Troy Luhman, Eric Luhman, Clarence Ng, Ricky Wang, and Aditya Ramesh. Video generation models as world simulators. 2024. 2, 1
- [5] Junsong Chen, Chongjian Ge, Enze Xie, Yue Wu, Lewei Yao, Xiaozhe Ren, Zhongdao Wang, Ping Luo, Huchuan Lu, and Zhenguo Li. Pixart- $\sigma$ : Weak-to-strong training of diffusion transformer for 4k text-to-image generation, 2024. 2
- [6] Junsong Chen, Yue Wu, Simian Luo, Enze Xie, Sayak Paul, Ping Luo, Hang Zhao, and Zhenguo Li. Pixart- $\delta$ : Fast and controllable image generation with latent consistency models, 2024.
- [7] Junsong Chen, Jincheng Yu, Chongjian Ge, Lewei Yao, Enze Xie, Yue Wu, Zhongdao Wang, James Kwok, Ping Luo, Huchuan Lu, and Zhenguo Li. Pixart- $\alpha$ : Fast training of diffusion transformer for photorealistic text-to-image synthesis. In *International Conference on Learning Representations*, 2024. 2, 5, 6, 1
- [8] Pengtao Chen, Mingzhu Shen, Peng Ye, Jianjian Cao, Chongjun Tu, Christos-Savvas Bouganis, Yiren Zhao, and Tao Chen.  $\delta$ -dit: A training-free acceleration method tailored for diffusion transformers. *arXiv preprint arXiv:2406.01125*, 2024. 2, 3, 6
- [9] Tri Dao, Daniel Y. Fu, Stefano Ermon, Atri Rudra, and Christopher R’e. Flashattention: Fast and memory-efficient exact attention with io-awareness. *ArXiv*, abs/2205.14135, 2022. 2, 5, 6, 8
- [10] Jia Deng, Wei Dong, Richard Socher, Li-Jia Li, Kai Li, and Li Fei-Fei. Imagenet: A large-scale hierarchical image database. In *2009 IEEE conference on computer vision and pattern recognition*, pages 248–255. Ieee, 2009. 6
- [11] Gongfan Fang, Xinyin Ma, and Xinchao Wang. Structural pruning for diffusion models. *arXiv preprint arXiv:2305.10924*, 2023. 3
- [12] Kunyu Feng, Yue Ma, Bingyuan Wang, Chenyang Qi, Haozhe Chen, Qifeng Chen, and Zeyu Wang. Dit4edit: Diffusion transformer for image editing. 2024. 1
- [13] Yunhui Guo, Chaofeng Wang, Stella X. Yu, Frank McKenna, and Kincho H. Law. Adaln: A vision transformer for multidomain learning and predisaster building information extraction from images. *J. Comput. Civ. Eng.*, 36, 2022. 4
- [14] Jack Hessel, Ari Holtzman, Maxwell Forbes, Ronan Le Bras, and Yejin Choi. Clipscore: A reference-free evaluation metric for image captioning. *arXiv preprint arXiv:2104.08718*, 2021. 5
- [15] Martin Heusel, Hubert Ramsauer, Thomas Unterthiner, Bernhard Nessler, and Sepp Hochreiter. Gans trained by a two time-scale update rule converge to a local nash equilibrium. *Advances in neural information processing systems*, 30, 2017. 6
- [16] Jonathan Ho, Ajay Jain, and Pieter Abbeel. Denoising diffusion probabilistic models. *Advances in neural information processing systems*, 33:6840–6851, 2020. 1, 2, 3
- [17] Ziqi Huang, Yanan He, Jiashuo Yu, Fan Zhang, Chenyang Si, Yuming Jiang, Yuanhan Zhang, Tianxing Wu, Qingyang Jin, Nattapol Chanpaisit, et al. Vbench: Comprehensive benchmark suite for video generative models. In *Proceedings of the IEEE/CVF Conference on Computer Vision and Pattern Recognition*, pages 21807–21818, 2024. 5
- [18] PKU-Yuan Lab and Tuzhan AI etc. Open-sora-plan, 2024. 2
- [19] Yanyu Li, Huan Wang, Qing Jin, Ju Hu, Pavlo Chemerys, Yun Fu, Yanzhi Wang, Sergey Tulyakov, and Jian Ren. Snapfusion: Text-to-image diffusion model on mobile devices within two seconds. *Advances in Neural Information Processing Systems*, 36, 2024. 3
- [20] Tsung-Yi Lin, Michael Maire, Serge Belongie, James Hays, Pietro Perona, Deva Ramanan, Piotr Dollár, and C Lawrence Zitnick. Microsoft coco: Common objects in context. In *Computer Vision—ECCV 2014: 13th European Conference, Zurich, Switzerland, September 6–12, 2014, Proceedings, Part V 13*, pages 740–755. Springer, 2014. 5
- [21] Xingchao Liu, Chengyue Gong, et al. Flow straight and fast: Learning to generate and transfer data with rectified flow. In *The Eleventh International Conference on Learning Representations*, 2023. 3, 5
- [22] Cheng Lu, Yuhao Zhou, Fan Bao, Jianfei Chen, Chongxuan Li, and Jun Zhu. Dpm-solver: A fast ode solver for diffusion probabilistic model sampling in around 10 steps. *Advances in Neural Information Processing Systems*, 35:5775–5787, 2022. 3
- [23] Cheng Lu, Yuhao Zhou, Fan Bao, Jianfei Chen, Chongxuan Li, and Jun Zhu. Dpm-solver++: Fast solver for guided sampling of diffusion probabilistic models. *arXiv preprint arXiv:2211.01095*, 2022. 3, 5
- [24] Xinyin Ma, Gongfan Fang, Michael Bi Mi, and Xinchao Wang. Learning-to-cache: Accelerating diffusion transformer via layer caching. *arXiv preprint arXiv:2406.01733*, 2024. 2, 3

- [25] Xinyin Ma, Gongfan Fang, and Xinchao Wang. Deepcache: Accelerating diffusion models for free. In *Proceedings of the IEEE/CVF Conference on Computer Vision and Pattern Recognition*, pages 15762–15772, 2024. [3](#)
- [26] William Peebles and Saining Xie. Scalable diffusion models with transformers. In *Proceedings of the IEEE/CVF International Conference on Computer Vision*, pages 4195–4205, 2023. [1](#), [2](#), [5](#)
- [27] Robin Rombach, Andreas Blattmann, Dominik Lorenz, Patrick Esser, and Björn Ommer. High-resolution image synthesis with latent diffusion models. In *Proceedings of the IEEE/CVF conference on computer vision and pattern recognition*, pages 10684–10695, 2022. [1](#), [2](#), [3](#)
- [28] Pratheba Selvaraju, Tianyu Ding, Tianyi Chen, Ilya Zharkov, and Luming Liang. Fora: Fast-forward caching in diffusion transformer acceleration. *arXiv preprint arXiv:2407.01425*, 2024. [2](#), [6](#), [7](#), [1](#)
- [29] Yuzhang Shang, Zhihang Yuan, Bin Xie, Bingzhe Wu, and Yan Yan. Post-training quantization on diffusion models. In *Proceedings of the IEEE/CVF conference on computer vision and pattern recognition*, pages 1972–1981, 2023. [3](#)
- [30] Jascha Sohl-Dickstein, Eric Weiss, Niru Maheswaranathan, and Surya Ganguli. Deep unsupervised learning using nonequilibrium thermodynamics. In *International conference on machine learning*, pages 2256–2265. PMLR, 2015. [2](#)
- [31] Jiaming Song, Chenlin Meng, and Stefano Ermon. Denoising diffusion implicit models. In *International Conference on Learning Representations*, 2021. [3](#), [5](#)
- [32] Wentian Zhang, Haozhe Liu, Jinheng Xie, Francesco Facio, Mike Zheng Shou, and Jürgen Schmidhuber. Cross-attention makes inference cumbersome in text-to-image diffusion models. *arXiv preprint arXiv:2404.02747v1*, 2024. [6](#)
- [33] Xuanlei Zhao, Xiaolong Jin, Kai Wang, and Yang You. Real-time video generation with pyramid attention broadcast. *arXiv preprint arXiv:2408.12588*, 2024. [3](#), [6](#), [1](#)
- [34] Zangwei Zheng, Xiangyu Peng, Tianji Yang, Chenhui Shen, Shenggui Li, Hongxin Liu, Yukun Zhou, Tianyi Li, and Yang You. Open-sora: Democratizing efficient video production for all, 2024. [5](#), [6](#)
- [35] Chang Zou, Xuyang Liu, Ting Liu, Siteng Huang, and Linfeng Zhang. Accelerating diffusion transformers with token-wise feature caching. *arXiv preprint arXiv:2410.05317*, 2024. [2](#), [3](#), [4](#), [6](#), [7](#), [1](#)

# Accelerating Diffusion Transformers with Dual Feature Caching

## Supplementary Material

### 6. Experimental Details

In this section, more details of the experiments are provided.

#### 6.1. Model Configuration

As mentioned in 4.1.1, experiments on three models from different tasks, PixArt- $\alpha$ [7] for text-to-image generation, OpenSora[4] for text-to-video generation, and DiT[26] for class-conditional image generation, are presented. In this section, a more detailed hyperparameter configuration scheme is provided.

- **PixArt- $\alpha$** : The average cache cycle length is set to  $\mathcal{N} = 3$  with an average caching ratio of  $R = 70\%$  for ToCa[35], and  $\mathcal{N} = 3$  with  $\mathcal{R} = 25\%$  for the DuCa method to maintain a similar acceleration ratio. Additionally, in the FORA [28] scheme,  $\mathcal{N} = 2$ . Conservative caching steps are configured to occur on odd-numbered steps following fresh steps, while aggressive caching steps occur on even-numbered steps following fresh steps. The proportion of conservative caching steps across layers and steps is identical to that in ToCa[35].

- **OpenSora**: The average cache cycle length is  $\mathcal{N} = 3$  for temporal attention, spatial attention, and MLP, and  $\mathcal{N} = 6$  for cross-attention, with an average caching ratio  $\mathcal{R} = 85\%$  exclusively for the MLP in ToCa[35] and DuCa, while all other modules use a caching ratio of 100%. In the FORA [28] scheme, all modules are set to  $\mathcal{N} = 2$ .

For **PAB<sup>1\*</sup>** [33], temporal attention is set to  $\mathcal{N} = 2$ , spatial attention to  $\mathcal{N} = 4$ , cross-attention to  $\mathcal{N} = 6$ , and the MLP module is fully computed. For **PAB<sup>2\*</sup>** [33],  $\mathcal{N}$  is set to 3, 5, and 7 for temporal, spatial, and cross-attention, respectively. For **PAB<sup>3\*</sup>** [33],  $\mathcal{N}$  is set to 5, 7, and 9 for temporal, spatial, and cross-attention, respectively.

For DuCa, conservative caching steps are set on odd-numbered steps following fresh steps, while aggressive caching steps are set on even-numbered steps following fresh steps. The proportion of conservative caching steps across layers and steps is identical to that in ToCa[35].

- **DiT**: The average cache cycle length is set to  $\mathcal{N} = 4$  with an average caching ratio of  $R = 93\%$  for ToCa[35](a),  $\mathcal{N} = 3$  with  $R = 93\%$  for ToCa[35](b), and  $\mathcal{N} = 3$  with  $R = 95\%$  for both DuCa(a) and (b). Additionally, the average cache cycle length for FORA [28] is set to  $\mathcal{N} = 3$ . Furthermore, for DuCa(a), conservative caching steps are set on even-numbered steps following fresh steps, while aggressive caching steps are set on odd-numbered steps. In contrast, for DuCa(b), the arrangement is reversed.

Since the average cache cycle length  $\mathcal{N} = 3$  here,

DuCa(a), which places aggressive caching steps immediately after the fresh step, achieves a higher acceleration ratio compared to DuCa(b), which places conservative caching steps in the first position after the fresh step.

#### 6.2. Anonymous Page for video presentation

To further demonstrate the superiority of DuCa in video generation, we have created an anonymous GitHub page. Please visit <https://duca2024.github.io/DuCa/> for a more detailed view. Besides, the videos are also available through the Supplementary Material.